AFRL-SR-AR-TR-06-0061

# REPORT DOCUMENTATION PAGE



| 1. AGENCY USE ONLY (Leave blank) | 2. REPORT DATE | 3. REPORT TYPE AND DATES COVERED |
|---|---|---|
| | 02-28-2006 | Final 05-01-2002 to 11-30-2005 |

**4. TITLE AND SUBTITLE**

## Creation of Metal and Semiconductor Nanostructures using DPN Nanolithography Techniques.

**5. FUNDING NUMBERS**

Grant # F49620-02-1-0188

**6. AUTHOR(S)**

Professor Jie Liu
Department of Chemistry
Duke University
Durham, NC 27708

**7. PERFORMING ORGANIZATION NAME(S) AND ADDRESS(ES)**

Duke University
327 North Building, Box
90077
Durham, NC 27708

**8. PERFORMING ORGANIZATION REPORT NUMBER**

**9. SPONSORING / MONITORING AGENCY NAME(S) AND ADDRESS(ES)**

AF Office of Scientific Research
801 N. Randolph Street, rm.732
Arlington, VA 22203
Jennifer Gresham/NL

**10. SPONSORING / MONITORING AGENCY REPORT NUMBER**

**11. SUPPLEMENTARY NOTES**

**12a. DISTRIBUTION / AVAILABILITY STATEMENT**

Approve for Public Release: Distribution Unlimited

**12b. DISTRIBUTION CODE**

**13. ABSTRACT** ***(Maximum 200 Words)***

Funds from AFOSR were used to support research activities on the fabrication and modification of nanoscaled structures using scanning probe microscope (SPM) based methods. Over the period of 3 and half years, significant progresses have been made to demonstrate the usefulness of SPM-based lithographic techniques. Major achievements include: 1) direct fabrication of polymeric nanostructures by initiating electrochemical polymerization directly under the SPM tips; 2)local chemical modification of existing nanostructures through local electrochemical reaction; 3) guided growth of polymeric nanostrucutres on surface patterns fabricated by SPM and other techniques; 4) growth of nanowires from catalyst islands fabricated from SPM based deposition method and 5) discovery of strong visible light emission from sulfur doped ZnO nanowires. These achievements not only expanded the scope of SPM based lithographic techniques that can be used to fabricate nanoscaled electronic devices for DOD applications as originally discussed in the proposal, some of the discoveries can also contribute to the development basic science beyond the scope of the original proposal. One example is the strong light emission from ZnO nanowires that can lead to the development of future LED light sources with high energy efficiency, saving significant amount of energy used for lighting.

| 14. SUBJECT TERMS | | | 15. NUMBER OF PAGES |
|---|---|---|---|
| | | | 16. PRICE CODE |
| 17. SECURITY CLASSIFICATION OF REPORT | 18. SECURITY CLASSIFICATION OF THIS PAGE | 19. SECURITY CLASSIFICATION OF ABSTRACT | 20. LIMITATION OF ABSTRACT |

NSN 7540-01-280-5500

Standard Form 298 (Rev. 2-89)
Prescribed by ANSI Std. Z39-18
298-102

Final Report (Grant # F49620-02-1-0188)

Grant Title: **Creation of Metal and Semiconductor Nanostructures using DPN Nanolithography Techniques.**

Jie Liu
Department of Chemistry
Duke University
Durham, NC 27708

Abstract:

Funds from AFOSR were used to support research activities on the fabrication and modification of nanoscaled structures using scanning probe microscope (SPM) based methods. Over the period of 3 and half years, significant progresses have been made to demonstrate the usefulness of SPM-based lithographic techniques. Major achievements include: 1) direct fabrication of polymeric nanostructures by initiating electrochemical polymerization directly under the SPM tips; 2)local chemical modification of existing nanostructures through local electrochemical reaction; 3) guided growth of polymeric nanostrucutres on surface patterns fabricated by SPM and other techniques; 4) growth of nanowires from catalyst islands fabricated from SPM based deposition method and 5) discovery of strong visible light emission from sulfur doped ZnO nanowires. These achievements not only expanded the scope of SPM based lithographic techniques that can be used to fabricate nanoscaled electronic devices for DOD applications as originally discussed in the proposal, some of the discoveries can also contribute to the development basic science beyond the scope of the original proposal. One example is the strong light emission from ZnO nanowires that can lead to the development of future LED light sources with high energy efficiency, saving significant amount of energy used for lighting.

## 1. Accomplishments

The focus of the research effort is the development and expansion of SPM based lithographic techniques, also called "Dip-pen" nanolithographic (DPN) methods. With the support from AFOSR, we were able to make significant progresses in several of the research directions related to the technology. Major achievements include: 1) direct fabrication of polymeric nanostructures by initiating electrochemical polymerization directly under the SPM tips; 2)local chemical modification of existing nanostructures through local electrochemical reaction; 3) guided growth of polymeric nanostrucutres on surface patterns fabricated by SPM and other techniques; 4) growth of nanowires from catalyst islands fabricated from SPM based deposition method and 5) discovery of strong visible light emission from sulfur doped ZnO nanowires. More detailed description of the achievements is the following:

1) Direct fabrication of polymeric nanostructures by initiating electrochemical polymerization directly under the SPM tips

SPL is an exciting research field that studies the modification of surfaces using Scanning Probe Microscopes (SPMs), including Scanning Tunneling Microscopes (STMs), Atomic Force Microscopes (AFMs) and Nearfield Scanning Optical Microscopes (NSOMs) etc. SPMs were invented as imaging tools in mid 1980s. The underlying mechanism for all SPMs is to move a sharp tip over a surface and monitor the changes in tunneling current between a metal tip and a conducting surface (in STM) or the deflection of a cantilever. Soon after, it was discovered that the tips used for imaging could also be used to modify the surfaces. Since then, many SPL techniques have been developed in the last decade based on various chemical, physical and electrical modification of surfaces, including mechanical scratching, electrochemical anodization of Si surfaces, decomposition of self-assembled monolayers, electric field induced chemical reactions, electrochemical reactions in solution using electrochemical STM tips etc.

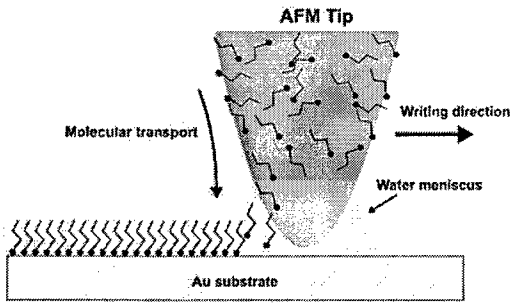


Figure 1. DPN of thiols on Au. From Piner et. al, Science 283, 661.

More recently, a new SPL technique, "dip-pen" nanolithography (DPN), has demonstrated the ability to pattern monolayer films of thiolated organic molecules with sub-100 nanometer resolution on gold substrates. The technology uses the spontaneous condensation between the AFM tip and substrate to transport organic molecules from the AFM tip to the surface in the area specifically defined by the tip/surface interaction. To draw a familiar analogy, the AFM tip acts as a "pen", the organic molecules act as "ink" and the surface acts as "paper" for nanostructures to be "drawn" on (Figure 1). It has also been demonstrated for direct patterning of nanoscale structures in both a serial and parallel fashion. This technique provides a potentially more accessible, cheaper, and versatile alternative to conventional high-resolution lithographic methods such as e-beam lithography.

**Precursor**

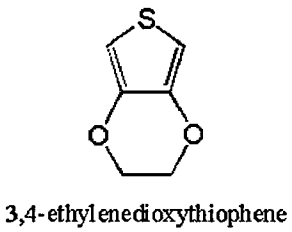

3,4-ethylenedioxythiophene

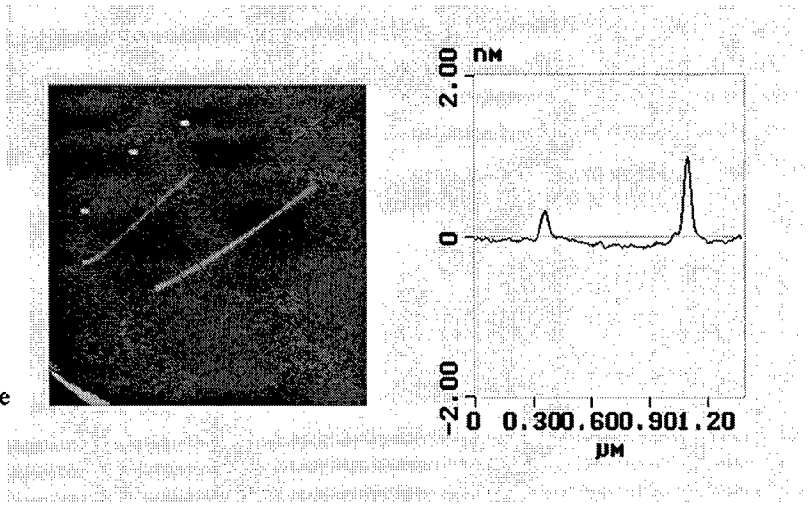


Figure 2. AFM image and height profiles of polymer lined drawn by E-DPN.

We have developed a new variation of the DPN method that also uses the tiny water meniscus on the AFM tip as the transfer medium. However, unlike the previous AFM "dip-pen" method where water is only used as a solvent for the molecules, we have used this tiny water meniscus as a nanometer-sized electrochemical cell in which metal salts can be dissolved, reduced into metals electrochemically and deposited on the surface. This is the first method that combines the versatility of electrochemistry with the simplicity and power of the DPN method to produce nanostructures with high resolution. Electrochemical STM based methods require that the substrates be metallic, but substrates used in our method do not have to be metallic since the control feedback of the AFM does not rely on the current between the tip and surface. Si wafers coated with a tin layer of native oxide provides enough conductivity for the reduction of the precursor ions. This development significantly expands the scope of DPN lithography, making it a more general nano-fabrication technique that not only can be used to deliver organic molecules onto surfaces, but is also capable of fabricating metallic and semiconducting structures with precise control of location and geometry. Because of the electrochemical nature of this new approach, we call this technique electrochemical "dip-pen" nanolithography (E-DPN).

We have shown that many metals and semiconductors can be deposited to the surface through electrochemical reduction of their water-soluble salts, including Pt, Au, Ag, Cu, Pd etc. The linewidth range from 30 nm to a few hundred nanometers depending on the relative humidity in the air, the applied voltage and scan rate of the AFM tips.

With the help of funds fromAFOSR, we have also shown that E-DPN method can be used to create conducting polymer nanostructrues. Many conducting polymers, including polypyrroles and polythiophenes, can be polymerized electrochemically. To create nanostructures of conducting polymers using DPN, we need to identify the right monomers or short polymer precursors that have the right solubility in water. We will coat the AFM with the precursor, adjust the distance between the AFM tips and the surface so the water meniscus can be formed. And then we will apply a negative bias to the tip so the monomers can be polymerized on the surface.

As shown in Figure 2, we have used 3,4-ethylenedioxythiophene as the precursor. The monomer can be polymerized on surfaces and nanoscale features with <100nm resolution can be created.

There are many advantages of using DPN to create nanoscale conducting polymer structures compare with other lithographic methods. In addition to the flexibility and simplicity that are true for all DPN methods, the conducting polymer structures can be locally doped with other organic molecules that can be deposited at specific locations on the structure with AFM. Since the conductivity and other properties such as the photoluminescence properties of the polymer chain are very sensitive to chemical doping, we can create functional structures like diode and light emitting devices using the technique. In addition, because of the virtually unlimited possibility of different monomers we can choose, we can create many different structures that are suitable for a wide variety of applications.

Though these techniques have been demonstrated for a few examples, the approach can be more general. In principle, if one can design a system with one reactant immobilized on the surface and the other delivered by the AFM tip to a specific location to perform chemical reactions, nanometer scale structures can be created as long as the reaction product is insoluble in water. One could envision using this technique to create nanostructures of other materials, modify existing nanostructures or measure the local chemical properties of the surface.

*Publications related to this research:*


- "Direct-writing of polymer nanostructures: Poly(thiophene) nanowires on semiconducting and insulating surfaces", B.W. Maynor, S.F. Filocamo, M.W. Grinstaff and J. Liu, *Journal of the American Chemical Society*, **124**(4), 522-523(2002).


2) Local chemical modification of existing nanostructures through local electrochemical reaction

Solid-state heterostructures are an integral part of the modern electronic and electro-optic device landscape. They are responsible for a variety of important electronic properties, including p-n junction current rectification and electroluminescence, avalanche breakdown in superlattice structures, and quantum-well emission in some types of laser diodes. As the miniaturization of electronic devices continues toward the nanometer regime, it is very important to find new ways to produce nanoscale analogs of metal-metal, metal-semiconductor or semiconductor-semiconductor heterostructures. Several groups have reported the synthesis of nanowire heterostructures using a variety of methods and materials. Many of these nanoscale heterostructures have been shown to posses a variety of interesting and technologically relevant properties, including rectification, luminescence, and negative differential conductance. The success in synthesizing these types of materials and the demonstration that they possess important electronic properties suggests that nanowire heterostructures will play a significant role in future nanoelectronic devices.

We have recently developed a new method for site-specific, Atomic Force Microscope (AFM) fabrication of nanowire heterostructures using Electrochemical Dip-Pen Nanolithography (E-DPN). E-DPN and other AFM lithography techniques can be used to modify surfaces in a rational manner by simply repositioning

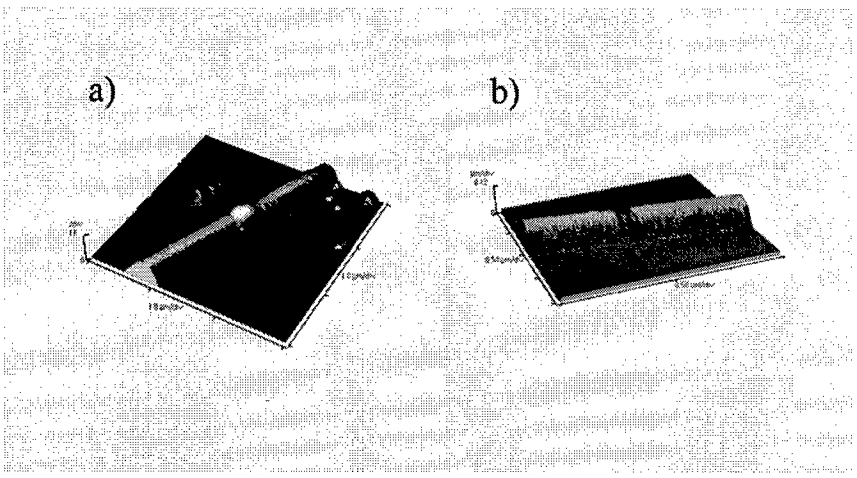


Figure 3. Representative AFM surface images of a GaN/gallium oxide heterostructure a) before and b) after selective etching in 1M HCl. The modification in (a) was performed at 40% humidity, 10 V surface-tip bias voltage, 30 sec dwell time. The modification in (b) was performed at 50% humidity, 10V surface-tip bias, 10 sec dwell time. The image in a) is 3 μm x 3 μm image and the image in b) is a 2 μm x 2 μm image.

the tip and chemically altering the surface using lithography. We have chosen E-DPN for a proof-of-concept study because it is ideally suited for the in-situ modification of nanoscale electronic devices; the AFM tip and the nanowire device can be used as electrodes and the reactants for the modification can be introduced by coating them onto the AFM tip. Specifically, we have created GaN nanowire heterostructures by a local electrochemical reaction between an n-type GaN nanowire and a tip-applied KOH "ink" to produce gallium nitride/gallium oxide heterostructures (Figure 3). By controlling the ambient humidity, reaction voltage, and reaction time, good control over the modification geometry is obtained. Furthermore, after selective chemical etching of gallium oxide, unique diameter-modulated nanowire structures can be produced. We have also demonstrated the unique device fabrication capabilities of this technique by performing in-situ modification of GaN nanowire devices and characterizing the device electronic transport properties. These results demonstrate that small modifications of nanowire devices can lead to large changes in the nanowire electronic transport properties.

We have also demonstrated that these unique heterostructures possess radically different electronic properties than the original GaN nanowires because the modification creates electronic transport barriers. Using this AFM-based methodology, it is possible to create many types of structures, including single-barrier and superlattice heterostructures simply by moving the ink-coated AFM tip to desired locations and modifying the nanowire by applying an appropriate bias voltage for a desired length of time. In addition to the modification of GaN, this modification scheme should also be applicable for other semiconductor nanowires such as CdS or InP. This E-DPN modification scheme provides a convenient means to deliver chemicals to specific locations on an existing nanostruture to perform chemical and structural modification. We believe it will have broad

applications in the creation of unique nanostructures/devices for the understanding of electronic transport in nanoscale junctions and size-modulated nanostructures. Future directions of research in this area will be the fabrication of complex functional nanodevices and the study of the relationship between the structure and electronic behavior.

*Publications related to this research:*

- Site-Specific Fabrication of Nanorod Heterostructures: Local Modification of GaN Nanowires using Electrochemical Dip-Pen Nanolithography, Benjamin W. Maynor, Jianye Li, Chenguang Lu, and Jie Liu, *Journal of the American Chemical Society,* **126**(20), 6409-6413 (2004)
- Controlled Growth of Long GaN Nanowires from Catalyst Patterns Fabricated by "Dip-Pen" Nanolithographic Techniques Jianye Li, Chenguang Lu, Benjamin Maynor, Shaoming Huang, and Jie Liu, *Chemistry of Materials*, **16**(9), 1633-1636 (2004).

3) Guided growth of polymeric nanostrucutres on surface patterns:

Conducting polymers (CPs), have been demonstrated to have very useful properties for electroluminescent devices, field effect transistors, and chemical sensors. These electronic properties are tunable by modification of the chemical structure of the monomer units, allowing the broad knowledge of organic chemistry to be applied to bandgap engineering. The impact of CPs in the field of electronics is expected to be great, due to this versatility, their mechanical flexibility, and their potential for extremely low cost device fabrication. Unlike inorganic semiconductor devices, CP devices do not have the expensive requirement of extreme environment control. Also, they have the potential to be used in inkjet printing for low cost circuit fabrication, which is very attractive for the electronic industry. However, this also imposes the restriction that patterned polymers be solution- or melt-processable. As a class of compounds, however, many CPs tend to be insoluble, and intractable in general, in their conducting states. Functionalization of the polymer with moieties to increase solubility, such as in Poly(3,4-ethylenedioxythiophene), is effective for achieving processability, but these substituents also alter the electronic properties, which is often undesirable.

We have recently developed a method to pattern CP nanostructure devices using a grow-in-place vapor-phase procedure that guides growth of polymer by selective condensation on a chemically patterned substrate. While previous efforts have used hydrophilic patterning, and even selective condensation to pattern a final CP structure, this is, to our knowledge, the first time such patterning has been used to directly grow devices in the submicron range.

Dendritic polymer structures were electrochemically grown between micropatterned electrodes from a monomer vapor. The growth was shown to require a critical value of relative humidity during growth, suggesting that a condensed layer of water on the surface of the sample is needed for polymerization. The accepted mechanism for polymerization of heterocycles such as pyrrole and thiophene involves elimination of protons, and electrochemical studies have found that the presence of some amount of protic solvent is helpful for growth of high-quality polymer. Solvent condensation on a surface is dependent on the affinity of the surface for that solvent, which in turn is dependent on the surface functionalization. At ambient temperatures and humidities, a small amount of water will be absorbed on a hydrophilic region of a substrate, but not on the adjacent hydrophobic regions. Many systems and techniques for patterning the hydrophobic/hydrophilic structures on a surface exist, including techniques that are compatible with well-developed methods in the semiconductor industry. Thus, the creation of CP nanostructures using the reported method can use both ultra-high resolution techniques such as e-beam or AFM lithography (< 10 nm feature size) and highly parallel methods such as photolithography (wafer-scale patterning in a single step).

Polymer growth across an electrode gap on bare silica was widespread, and not confined to the smallest electrode gap (Figure 4a). In control experiments, HMDS functionalization of the silica surfaces prevented

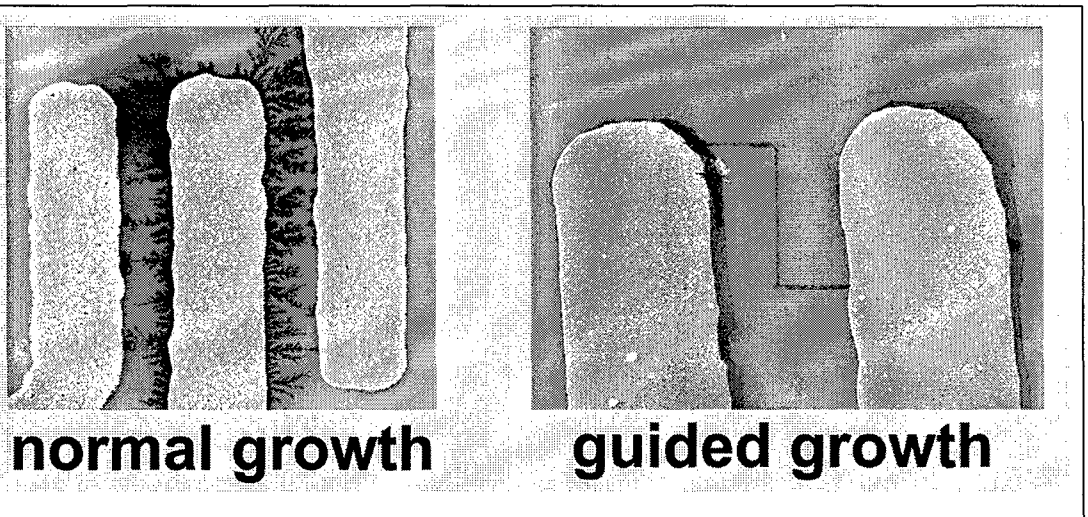


Figure 4. SEM images of conducting polymer grown on bare $SiO_2$ surface and on patterned $SiO_2$ surface

polymer growth even after over 12 hours of applied bias. Hydrophilic surface patterning was successful in confining polymer growth to a small predefined area. (Fig. 4b) The size of the polymer structures matched the size of the modified area on which they were grown. Polymer structures were fibrillar, with individual chains 10 to 30 nm thick, as measured by AFM. The fibril density increased with growth time, but very thin films (no more than 20 nm thick) were almost always grown. It was found that anionic dopants, introduced intentionally, or present as impurities, were necessary to grow conductive structures. Structures grown with only surface impurities exhibited low conductivities and poor reproducibility. Thus, a controlled method to provide dopant species was needed. HCl is mobile in the vapor phase, and dissociates in water to give $Cl^-$ ions, which have been shown to dope polypyrrole. We therefore repeated the growth procedure in the presence of 6M HCl. Polypyrrole structures grown in this way displayed much higher growth rates, more ordered structures, and

conductivities more than three orders of magnitude higher than those of comparable samples doped only by impurities. Growth progress was monitored through measurement of electric resistance across the electrodes. Resistance dropped steadily in most cases, but suddenly for some highly-doped samples. A steady decrease suggests a slow increase in the diameter of poorly conducting, very thin polymer fibers, while a sudden drop suggests a thicker fiber has just bridged the electrode gap.

For electronic transport in conducting polymers, charge carrier availability and carrier delocalization are both required. Charge carriers are introduced to the polymer structures by oxidation of monomer units within the polymer chain. Typically, this oxidation proceeds up to a maximum percent doping, where a fraction of the total number of monomer units has been oxidized. When this maximum is reached, the polymer will conduct as a metal, and will display no gate dependence. However, at doping levels with low carrier concentrations, an external electric field can introduce charge carriers, and control polymer conductivity. Thus, the growth method can be used to create both metallic and semiconducting structures. In the case of lightly-doped polypyrrole, the electric-field sensitivity is that of a p-type semiconductor. Gate dependences seen in the samples doped only by impurities, however, were weak. This is due to the relatively poor charge delocalization of the samples grown at low doping levels. Conductivities for these samples were usually in the range of 0.0001 S/cm, even after post-growth doping. Semiconducting samples of higher quality were produced from highly doped samples grown in the presence of HCl, with maximum conductivities around 0.1 S/cm. These samples were then electrochemically reduced, and the $Cl^-$ dopants removed, reducing the available charge for transport, while retaining the carrier delocalization properties. After this, the samples gave well-defined gate curves. Conductivities of the polymer structures created in this study were lower than those reported for bulk synthesis methods. This problem could probably be solved by fine-tuning the growth conditions such as temperature, monomer and dopant concentration, or electrochemical potential. These growth conditions have been shown to have a large effect on the conductivity and mobility of the polymer, so significant improvement of the performance of grown structures can be expected.

Here,we have demonstrated a versatile method for patterning polypyrrole with high resolution, complex geometry, control over electrical properties, and superior orientation compared to other synthesis methods. Because the growth is confined to a surface pattern, semiconductor devices with relatively high performance can theoretically be made. If the guided growth process can be generalized to parallel surface patterning methods such as photolithography, the low-cost potential of CP devices can be retained. Further, the polymer fibers are grown in alignment with the direction of electrical transport, something which is impossible for all CP device fabrication methods other than electrochemical growth. Future experiments exerting more control over the electrochemical environment of the polymerization reaction are expected to yield devices with better structure and delocalization, improving properties in both the metallic and semiconductor modes. If this is realized, guided growth can have great potential for fabrication of CP electronics.

*Publications related to this research:*

- "Guided Growth of Nanoscale Conducting Polymer Structures on Surface Functionalized Nanopatterns", Michael Woodson, Jie Liu, *Journal of American Chemical Society*, Available as ASAP article (2006), http://pubs.acs.org/cgi-bin/asap.cgi/jacsat/asap/html/ja057500i.html.

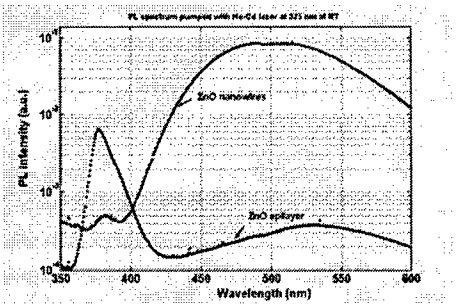


Figure 5. PL Spectrum of ZnO nanowires and epilayers. The Y-axis is in log scale.

4). Strong white light emission from ZnO nanowires

Study on nanowires of semiconducting materials has been an active research area in the last decade. Many different kinds of nanowires, nanobelts, nanoribbons etc. have been synthesized and studied. However, most of the current research on the applications of the materials focuses on nanoscale electronic and optical devices using individual nanowires. For example, nanoscale lasers and waveguides using ZnO nanowires have been made; chemical and biological sensors made of individual nanowires were also demonstrated. Although the miniturization of devices is a very important task for researchers in this field, nanoscale materials can offer much more than just the size reduction. Unique properties possessed by nanoscaled materials that are not observed in their bulk form provide many exciting research opportunities. Understanding and utilizing these properties will enable new and important applications.

Over the last year, we have discovered that certain ZnO nanowires emit strong broadband light in visible region. The spectrum matches so well to the dark adapted Human Visual Sensitivity (Human eye sensitivity under low light conditions) curve, that makes the material best suited for nighttime lighting. There are many distinct advantages for using ZnO nanowires for white light generation, including:

*High energy efficiency.* ZnO is known for its high quantum efficiency compare with other wideband gap semiconductors (GaN, SiC). The materials can be used as phosphor in combination with existing UV light LED to generate white light or be made into a white LED directly. Although white LED light source exist now, most commercial "white" LED gives a bluish light;

Low cost and scalable production: The production of ZnO nanowires is simply heating ZnO and/or ZnS powder to high temperature and let them condense on Si wafer coated with various catalysts;

*Stability and long lifetime.* Unlike materials like GaN which slowly oxidize in air and introduce defects in the material over time, ZnO does not oxidize in air since it is already an oxide. It may not be necessary to seal the device in vacuum or inert gas container, further reducing the cost of the lighting devices;

*Environmentally friendly.* ZnO materials have been used in dietary and cosmetic products for many years already; Although there were recent reports from Sadia National Lab that use quantum dots as phosphors coating blue LED to generate white light, the materials, CdSe, CdS etc. are toxic and environmentally unfriendly, making them not suitable for applications in environment with intense human activities.

We believe the observed strong and broadband emission from ZnO nanowires present a unique opportunity offered by nanoscale materials. The continued study and development of a white light source based on this material will greatly enhance our understanding of the photonic properties of nanoscaled materials and contribute to the development of energy efficient light sources for daily use, saving significant amount of our precious energy source.

*Synthesis of Long ZnO/ZnS nanowires and nanobelts.*

Methods to synthesis various ZnO nanostrunctures were developed in our lab. ZnO nanowires can be synthesized using ZnO powder as source and Au, Fe, Ni nanoparticles as catalysts. Ultra-long wurtzite structure ZnO nanowires and nanobelts were grown by a ZnO powders sublimation method. Various other ZnO nanostructures can also be obtained. The structures include: nanorings, nanosprings, nanonails, nanobrooms, nanoforks etc.

*Photoluminescence study of GaN and ZnO nanowires*

Typical ZnO bulk materials or thin films have very strong UV emission around 3.3 eV at room temperature with faint green emission at 2.4 eV (Figure 5, blue curve). This green emission is typically attributed to O vacancy or Zn interstitials in many reports. For ZnO nanowires, literatures show similar optical properties. However, for several ZnO nanowire samples grown using gold catalyst we have studied, the green emission become very strong and reach an intensity five order of magnitude higher than its band edge UV emission. However, for ZnO nanowires grown using other catalysts, the PL intensities for green and band edge emission are comparable.

The origin of such strong enhancement in luminescence efficiency is not clear presently. Especially when the luminescence centers are thought to be defects or defect complexes. The understanding of such origin is the main goal of the ongoing research. A manuscript is recently submitted to *Nano Letters.*

*Publications related to this research:*

- "Time-resolved Investigation of Bright Visible Wavelength Luminescence from Sulfur-doped ZnO Nanowires and Micropowders", John V. Foreman, Jianye Li, Hongying Peng, Soojeong Choi, Henry O. Everitt and Jie Liu, Submitted to *Nano Letters* (2006)

**2. Personnel Supported**:

Mr. Michael Woodson (Graduate Student)

Dr. Jianye Li (Postdoc)

Mr. Qiang Fu (Graduate Student)

**3. Publications:**

1. "Direct-writing of polymer nanostructures: Poly(thiophene) nanowires on semiconducting and insulating surfaces", B. W. Maynor, S. F. Filocamo, M. W. Grinstaff and J. Liu,*Journal of the American Chemical Society*, 124 (4), 522-523 (2002).
2. "A simple method for the synthesis of highly oriented potassium-doped tungsten oxide nanowires", H. Qi, C. Y. Wang and J. Liu, *Advanced Materials*, 15 (5), 411-+ (2003).
3. "Controlled growth of long GaN nanowires from catalyst patterns fabricated by "Dip-Pen" nanolithographic techniques", J. Y. Li, C. G. Lu, B. Maynor, S. M. Huang and J. Liu, *Chemistry of Materials*, 16 (9), 1633-1636 (2004).
4. "Site-specific fabrication of nanoscale heterostructures: Local chemical modification of GaN nanowires using electrochemical dip-pen nanolithography", B. W. Maynor, J. Y. Li, C. G. Lu and J. Liu, *Journal of the American Chemical Society*, 126 (20), 6409-6413 (2004).
5. "Creation of Cadmium Sulfide Nanostructures Using AFM Dip-Pen Nanolithography", Lei Ding, Yan Li, Haibin Chu, Xuemei Li, and Jie Liu, *Journal of Physical Chemistry B*, 109(47); 22337-22340, (2005).
6. "Conversion between Hexagonal GaN and β-$Ga_2O_3$ Nanowires and Their Electrical Transport Properties", Jianye Li, Lei An, Chenguang Lu, and Jie Liu, *Nano Lett.*, 6 (2), 148 -152 (2006).
7. "Guided Growth of Nanoscale Conducting Polymer Structures on Surface Functionalized Nanopatterns", Michael Woodson, Jie Liu, *Journal of American Chemical Society*, Available as ASAP article (2006), http://pubs.acs.org/cgi-bin/asap.cgi/jacsat/asap/html/ja057500i.html.
8. "Time-resolved Investigation of Bright Visible Wavelength Luminescence from Sulfur-doped ZnO Nanowires and Micropowders", John V. Foreman, Jianye Li, Hongying Peng, Soojeong Choi, Henry O. Everitt and Jie Liu, Submitted to *Nano Letters* (2006)

**4. New Discoveries, Inventions or Patent disclosures:**

1. Zinc Oxide Nanowires for Broad Visible Light Generation and Their Applications in General Lighting, Jianye Li, Hongying Peng, Henry Everitt, Jie Liu, Pending, Filed in 2005.

**5. Honors/Awards:**

Jie Liu received 2002 Dupont Young Professor Award from Dupont and 2002 Outstanding Oversea Young Investigator Award from NSF-China.

**Appendix:**

1. Manuscript submitted to Nanoletters on light emission from ZnO nanowires;

# Time-resolved Investigation of Bright Visible Wavelength Luminescence from Sulfur-doped ZnO Nanowires and Micropowders

*John V. Foreman*[†,‡], *Jianye Li*[§], *Hongying Peng*[†,⊥], *Soojeong Choi*[†], *Henry O. Everitt*[*,†,‡] *and Jie Liu*[*,§]

Department of Chemistry and Department of Physics, Duke University, Durham, North Carolina 27708, and U.S. Army Aviation & Missile Research, Development & Engineering Center, Redstone Arsenal, Alabama 35898

[*]Corresponding Authors. Email: everitt@phy.duke.edu. Email: jliu@chem.duke.edu.

**RECEIVED DATE (to be automatically inserted after your manuscript is accepted if required according to the journal that you are submitting your paper to)**

[†]Department of Physics, Duke University; [‡]Aviation & Missile RDEC; [§]Department of Chemistry, Duke University; [⊥]Present address: GE Global Research Center, Niskayuna, New York

ABSTRACT: Sulfur-doped zinc oxide (ZnO) nanowires grown on gold-coated silicon substrates inside a horizontal tube furnace exhibit remarkably strong visible wavelength emission with a quantum efficiency of 30%, an integrated intensity 1,600 times stronger than band edge ultraviolet emission, and a spectral distribution that closely matches the dark-adapted human eye response. By comparatively studying sulfur-doped and undoped ZnO micropowders, we clarify how sulfur doping and nanostructuring affect the visible luminescence and the underlying energy transfer mechanisms.

MANUSCRIPT TEXT:

Increasing interest in the optoelectronic properties of wide band gap semiconductor materials, heterostructures, and nanostructures is largely motivated by the need to develop bright emitters and phosphors in the ultraviolet and visible wavelength regions. In spite of the commercial success of the III-V gallium nitride (GaN) material system, interest in the II-VI semiconductor zinc oxide (ZnO) was renewed in the late 1990s when room-temperature, optically pumped lasing was demonstrated for ZnO thin films.[1-5] Since that time the optical properties of ZnO bulk single crystal, thin films, and nanostructures have been studied extensively. Frequently cited advantages of ZnO over GaN include a larger exciton binding energy[6,7] (60 meV vs. 26 meV), the availability of high-quality single-crystal ZnO substrates, amenability to chemical etching, resistance to oxidation, environmental friendliness, and lower cost. Progress is even being made toward establishing reproducible methods for p-doping ZnO.[8-12]

The other outstanding issue related to optoelectronic applications of ZnO is improved material quality, often characterized by the degree of broad, defect-related "green band" or "visible band" emission (centered at ~2.5 eV) that almost always accompanies the ultraviolet (UV) band edge emission (~3.3 eV at 295 K). In bulk ZnO and in thin films of sufficient quality, the intensity of visible emission is several orders of magnitude weaker than that of the band edge emission.[13-16] For ZnO nanostructures, however, the intensity of the defect emission can be much stronger. Indeed, the peak intensity ratio ($\equiv I_D^{Peak} / I_B^{Peak}$) of the defect emission to the band edge emission has been reported as large as 10, but because the visible emission is broader, the spectrally integrated ratio ($\equiv I_D / I_B$) is as large as 40.[17-20] Furthermore, it is well established that sulfur doping enhances the visible emission from ZnO nanowires, with $I_D / I_B \leq 22$ at room temperature[21,22] and $I_D / I_B \sim 1500$ at 10 K.[23] In these reports it has been suggested that sulfur substitutes for oxygen within the ZnO lattice, and the enhanced visible emission is due to the commensurate increase in oxygen vacancies.

The chemical and structural origins of the visible luminescence from *undoped* ZnO are still a matter of debate. In what is perhaps the most frequently cited explanation,[24] electrons trapped at singly ionized

oxygen vacancies recombine with valence band holes. In another frequently cited explanation,[25] electrons in the conduction band and/or shallow donor states recombine with holes which have been trapped at oxygen vacancies. The significant contribution of surface defects to visible emission is evident from the observation that $I_D^{Peak} / I_B^{Peak}$ is much higher in ZnO nanostructures than in bulk or thin films due to the nanostructures' increased surface-to-volume ratio. Indeed, recent work by Shalish *et al.* demonstrated that the intensity of defect emission in an array of ZnO nanowires was directly proportional to the wires' average surface-to-volume ratio.[20] Measurements of the polarization of band edge versus defect emission[18] and studies involving surfactant treatments in ZnO nanostructures[26,27] also indicate that the visible emission originates from the surfaces of these materials, thus lending further support to the claim that surface defects are primarily responsible for the visible emission.

In this letter, we seek to understand the comparative roles of sulfur doping and nanostructuring in the desirable generation of defect emission from ZnO nanowires for their use as a possible UV-excited phosphor producing bright, efficient, and broad visible-wavelength light. To wit, we report the growth and characterization of sulfur-doped ZnO nanowires and micropowders whose integrated visible emission is broad and more than *three orders of magnitude* brighter than the band edge UV emission. By using time resolved photoluminescence techniques, the efficient energy transfer from bulk to defect is observed, and the roles of nanostructuring and sulfur doping in producing visible emission are assessed. In contrast to previous reports of greater visible emission with increasing surface-to-volume ratio in ZnO, we find that nanostructuring sulfur-doped ZnO introduces nonradiative relaxation pathways that reduce the visible luminescence efficiency.

The ZnO:S nanowires were grown on gold-coated silicon substrates inside a horizontal tube furnace. Zinc sulfide (ZnS) and carbon (C) were used in a weight ratio of 2:1 as starting materials. Due to trace amounts of oxygen in the argon carrier gas, the zinc is oxidized and S-doped ZnO nanowires are formed. Further details of the growth procedure can be found in the Supporting Information. To ascertain the relative effects of doping and nanostructuring on the optical properties of the nanowires, we compared the emission of the nanowires to that of micrometer-scale ZnO powder in both undoped

and sulfur-doped forms. The commercially available, undoped powder was obtained from Aldrich, and a portion of this "micropowder" was sealed with small amount of sulfur in a quartz tube and annealed at 1000 °C for one hour to produce ZnO:S powder.

The optical properties of the samples were characterized using standard spectroscopic equipment. A HeCd laser operating at 3.81 eV (325 nm) was used for continuous-wave excitation, and the 100 fs pulsed output of a 1 kHz optical parametric amplifier, tuned to the same energy, was used for pulsed excitation during the time-resolved measurements. Further details of the optical setup are provided in the Supporting Information.

Figure 1 shows X-ray diffraction (XRD) and scanning electron microscope (SEM) data for one of the nanowire samples. The strong diffraction peaks in Figure 1A correspond to ZnO. Two small peaks corresponding to ZnS are also observed, indicating the existence of a small amount of ZnS impurity in the material. The SEM images in Figure 1B indicate that the wires are very long (~20 μm) and uniform along their length, with average cross sections of ~500 x 150 $nm^2$. SEM data (not shown) for the micropowder samples indicate that the average particle diameter is ~125 μm.

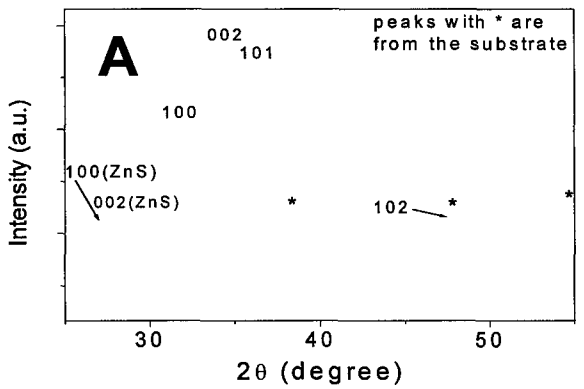

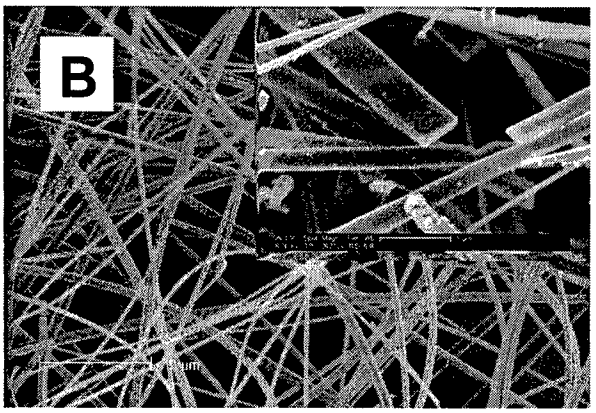


***Figure 1.*** *(A) All significant peaks in the XRD data for the nanowires can be indexed to ZnO. (B) SEM images for the sulfur-doped ZnO nanowires indicate that the wires are very long and uniform along their length, with average dimensions 500 nm x 150 nm x 20 μm.*

The room temperature, continuous-wave photoluminescence (PL) spectra of spontaneous emission from the sulfur-doped ZnO nanowires, the commercially available undoped ZnO micropowder, and a sulfur-doped portion of the powder are shown in Figure 2A. The broad emission spectra of the sulfur-doped ZnO nanowires and micropowders very closely match the dark-adapted response[28] of the human eye. Moreover, their brightness and large spectrally integrated quantum efficiencies (30% and 65%, respectively) make them compelling UV-excited phosphors. There have been no prior measurements of the quantum efficiency of *defect* emission from ZnO nanostructures, although a band edge quantum efficiency of approximately 10% has recently been reported for spontaneous emission of undoped ZnO nanowires.[29] The 65% quantum efficiency of the S-doped ZnO powder is consistent with a previously reported value of 60%.[30]

To ascertain what wavelength of UV excitation most efficiently produces the green emission, photoluminescence excitation (PLE) spectroscopy was performed on the doped nanowire and micropowder samples (Figure 2B). An excitonic resonance is clearly observed at 3.30 eV in the absorption profiles, indicating that excitation at the free exciton ground state energy maximizes the intensity of defect emission.

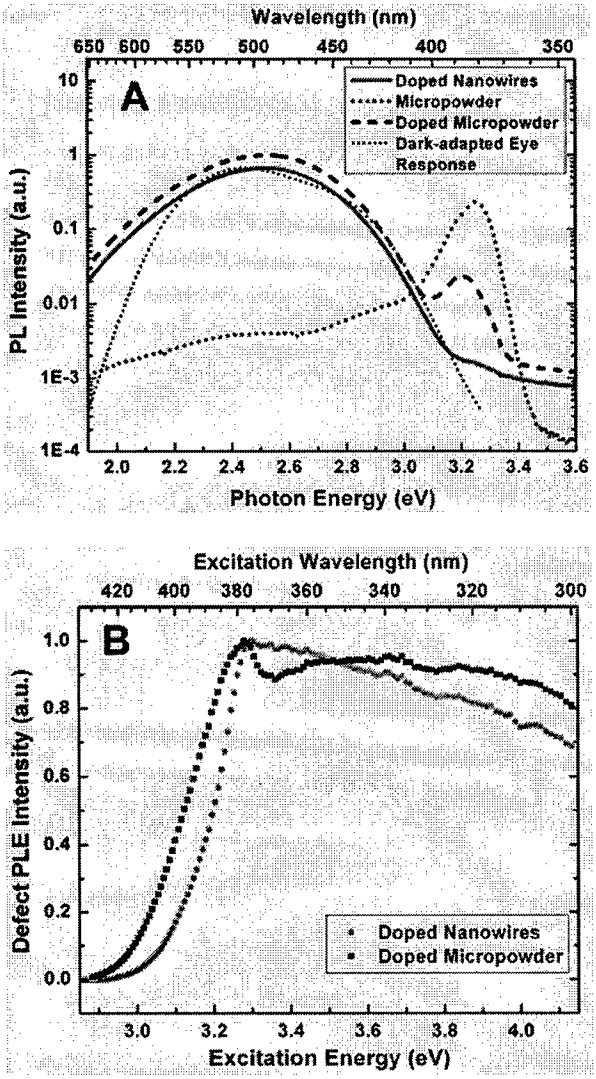


***Figure 2.*** *(A) Photoluminescence spectrum of ZnO nanowires and the very similar spectral response of the dark-adapted human eye.*[28] *The PL spectra of commercial ZnO micropowders (undoped and doped with sulfur) are shown for comparison. All spectra have been corrected for the samples' respective absorption. (B) Photoluminescence excitation spectra of the sulfur-doped materials for a detection energy of 2.5 eV. The spectra are normalized to the excitonic resonance at 3.30 eV.*

In general, the ratio of defect to band edge emission, $I_D / I_B$, depends on growth technique and can be increased through nanostructuring. However, the unprecedented $I_D^{Peak} / I_B^{Peak}$ of the doped nanowires reported here cannot be explained by nanostructuring alone. The analysis of Shalish *et al.* regarding

undoped ZnO nanowires[20] predicts $I_D^{Peak} / I_B^{Peak} = 0.3$ for an undoped version of our nanowires, not the $I_D^{Peak} / I_B^{Peak} = 400$ observed. We attribute the factor of ~1300 difference in these ratios to sulfur doping. By way of proof, we note that $I_D^{Peak} / I_B^{Peak}$ changes from 0.02 to 80 when comparing undoped to sulfur-doped micropowders—a factor of 4000 change. The similarity in intensity and spectral distribution of the entire broadband emission of the doped nanowires and micropowder (Figure 2A) suggests a common origin that is lacking for the undoped sample.

As noted above, there is experimental evidence that the visible emission originates from surface states in both undoped[18,20,26,27] and sulfur-doped[21] ZnO. It is therefore somewhat unexpected that our sulfur-doped micropowders with small surface-to-volume ratio exhibit double the quantum efficiency and triple the improvement in $I_D^{Peak} / I_B^{Peak}$ compared to our sulfur-doped nanowires with larger surface-to-volume ratio. We posit that the greater surface-to-volume ratio in the sulfur-doped nanowires contributes a greater density of nonradiative traps that directly compete with the sulfur-mediated radiative relaxation.

| | **$I_D/I_B$** | **UV decay $\tau_1$ (ns)** | **UV decay $\tau_2$ (ns)** | **UV decay $A_1$** | **quantum efficiency** |
|---|---|---|---|---|---|
| Undoped micropowder | 0.08 | 0.198 | 1.08 | 0.48 | 7% |
| S-doped micropowder | 320 | 0.112 | 0.481 | 0.37 | 65% |
| S-doped nanowire | 1600 | <0.040 | - | - | 30% |

***Table 1.*** *TRPL biexponential decay characteristics of band edge emission for undoped and S-doped ZnO micropowders and nanowires.*

To confirm this hypothesis, we measured the time-resolved photoluminescence (TRPL) decay of the band edge and defect emission from each ZnO sample. First consider the decay of the band edge emission (Table 1 and Figure 3A).[31] The undoped micropowder exhibits the strongest band edge emission (and the weakest defect emission). Although it has the slowest biexponential decay lifetimes $\tau_i$ ($I_B(t) = A_1 e^{-t/\tau_1} + A_2 e^{-t/\tau_2}, A_1 + A_2 = 1$), the low quantum efficiency indicates that nonradiative recombination dominates band edge relaxation. Doping the micropowder with sulfur significantly enhances energy transfer from the band edge to the defect states responsible for visible emission, resulting in reduced band edge emission, faster band edge decay, much brighter visible emission, and dramatically increased quantum efficiency. Clearly the defect-mediated decay channel responsible for visible emission favorably competes with the deleterious nonradiative decay channels. However, when the doped ZnO is formed into nanowires, the band edge emission decay accelerates and the spectrally integrated quantum efficiency drops. Clearly nanostructuring increases nonradiative carrier relaxation, thus undermining the channel favorable for visible emission. It is surmised that as the nanostructure surface-to-volume ratio increases, the nonradiative pathways increasingly compete with the sulfur-induced defects responsible for the bright visible emission.

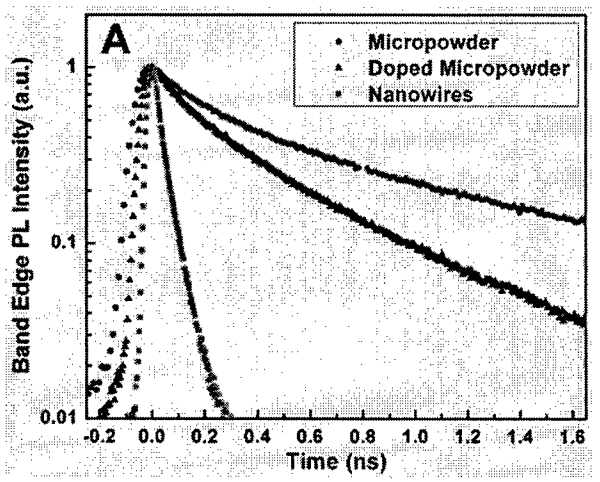

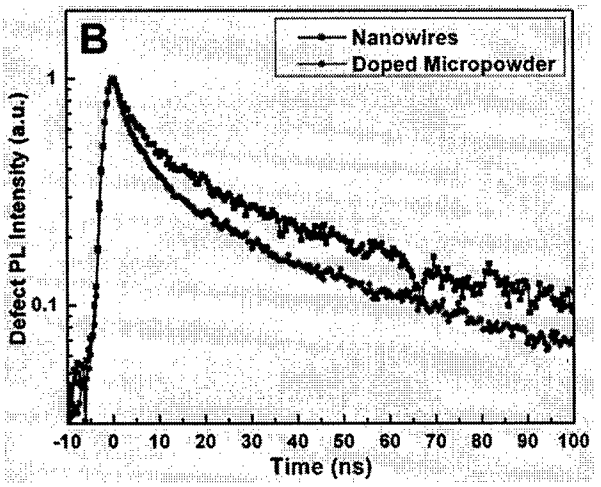


***Figure 3.*** *(A) Time-resolved, spectrally-integrated band edge photoluminescence of ZnO micro- and nanostructures. The large, undoped ZnO micropowder exhibits the most intense band edge emission and decays at the slowest rate. When thermally treated in a sulfur environment, the defect emission of the micropowder is significantly enhanced, and the band edge emission accelerates. The band edge decay of the ZnO nanowires is even faster (near the instrument resolution) due to the presence of many nonradiative recombination channels. (B) The complex and slow decay of visible wavelength emission from sulfur-doped ZnO micropowder and nanowires is revealed by spectrally integrated time-resolved photoluminescence spectroscopy.*

Next, consider the decay of the visible emission itself. The decay lifetimes were almost independent of emission wavelength across the broad visible emission band for both the doped micropowder and nanowire samples. This suggests a common emission mechanism that is enhanced by the presence of sulfur but is otherwise independent of sample preparation conditions. Figure 3B compares the spectrally integrated (2.27-2.77 eV) visible emission decay for both samples. The complex, nonexponential decay occurs on a timescale much longer than that of the band edge emission, decreasing to half its initial intensity in 10 ns. The final 10% of this emission decays exponentially with a time constant of ~50 ns. This may be compared with microsecond lifetimes previously reported in the literature for visible emission in undoped ZnO.[25,32] The similarity of the two TRPL traces indicates that

the nanostructuring process and commensurate increase in nonradiative relaxation pathways has little effect on the decay dynamics of the visible wavelength emitters themselves.

Understanding the mechanism of visible emission in ZnO nanostructures is necessary not only to minimize its effects in cases where band edge ultraviolet emission is important, but also to *enhance* the mechanism for the purpose of engineering bright emitters and phosphors in the visible spectrum. The sulfur-doped nanowires and micropowders discussed in this report are clearly a viable broadband light source which can be efficiently and continuously photoexcited by commercially available semiconductor UV emitters. Electrical pumping of the ZnO nanowires is also possible because of their comparatively high electrical conductivity. For phosphor applications, however, sulfur-doped ZnO powder is still preferable to nanowires because of large-quantity availability and lower cost.

**Acknowledgment.** This work was partially supported by the Army Research Office through grant number W011NF-04-D-0001/DI #0002 and by AFOSR through grant number #49620-02-1-0188.

**Supporting Information Available:** Experimental techniques and materials. This material is available free of charge via the Internet at http://pubs.acs.org.

**References**

(1) Bagnall, D. M.; Chen, Y. F.; Zhu, Z.; Yao, T.; Shen, M. Y.; Goto, T. *Appl. Phys. Lett.* **1998**, *73*, 1038-1040.

(2) Tang, Z. K.; Wong, G. K. L.; Yu, P.; Kawasaki, M.; Ohtomo, A.; Koinuma, H.; Segawa, Y. *Appl. Phys. Lett.* **1998**, *72*, 3270-3272.

(3) Zu, P.; Tang, Z. K.; Wong, G. K. L.; Kawasaki, M.; Ohtomo, A.; Koinuma, H.; Segawa, Y. *Solid State Comm.* **1997**, *103*, 459.

(4) Bagnall, D. M.; Chen, Y. F.; Zhu, Z.; Yao, T.; Koyama, S.; Shen, M. Y.; Goto, T. *Appl. Phys. Lett.* **1997**, *70*, 2230-2232.

(5) Reynolds, D. C.; Look, D. C.; Jogai, B. *Solid State Comm.* **1996**, *99*, 873.

(6) Reynolds, D. C.; Look, D. C.; Jogai, B.; Litton, C. W.; Cantwell, G.; Harsch, W. C. *Phys. Rev. B* **1999**, *60*, 2340.

(7) Xu, S. J.; Liu, W.; Li, M. F. *Appl. Phys. Lett.* **2002**, *81*, 2959.

(8) Tsukazaki, A.; Ohtomo, A.; Onuma, T.; Ohtani, M.; Makino, T.; Sumiya, M.; Ohtani, K.; Chichibu, S. F.; Fuke, S.; Segawa, Y.; Ohno, H.; Koinuma, H.; Kawasaki, M. *Nature Mater.* **2005**, *4*, 42-46.

(9) Look, D. C.; Claflin, B. *Phys. Stat. Sol. B* **2004**, *241*, 624-630.

(10) Kim, K.-K.; Kim, H.-S.; Hwang, D.-K.; Lim, J.-H.; Park, S.-J. *Appl. Phys. Lett.* **2003**, *83*, 63.

(11) Look, D. C.; Renlund, G. M.; Burgener II, R. H.; Sizelove, J. R. *Appl. Phys. Lett.* **2004**, *85*, 5269.

(12) Vaithianathan, V.; Lee, B.-T.; Kim, S. S. *Appl. Phys. Lett.* **2005**, *86*, 062101.

(13) Ozgur, U.; Teke, A.; Liu, C.; Cho, S. J.; Morkoc, H.; Everitt, H. O. *Appl. Phys. Lett.* **2004**, *84*, 3223-3225.

(14) Wang, L.; Giles, N. C. *J. Appl. Phys.* **2003**, *94*, 973.

(15) Leiter, F.; Alves, H.; Pfisterer, D.; Romanov, N. G.; Hofmann, D. M.; Meyer, B. K. *Physica B* **2003**, *340-342*, 201.

(16) Jung, S. W.; Park, W. I.; Cheong, H. D.; Gyu-Chul, Y.; Hyun, M. J.; Hong, S.; Joo, T. *Appl. Phys. Lett.* **2002**, *80*, 1924-1926.

(17) Greene, L. E.; Law, M.; Goldberger, J.; Kim, F.; Johnson, J. C.; Zhang, Y.; Saykally, R. J.; Yang, P. *Angew. Chem. Int. Ed.* **2003**, *42*, 3031.

(18) Hsu, N. E.; Hung, W. K.; Chen, Y. F. *J. Appl. Phys.* **2004**, *96*, 4671.

(19) Liu, X.; Wu, X.; Cao, H.; Chang, R. P. H. *J. Appl. Phys.* **2004**, *95*, 3141.

(20) Shalish, I.; Temkin, H.; Narayanamurti, V. *Phys. Rev. B* **2004**, *69*, 245401.

(21) Bae, S. Y.; Seo, H. W.; Park, J. *J. Phys. Chem. B* **2004**, *108*, 5206-5210.

(22) Geng, B. Y.; Wang, G. Z.; Jiang, Z.; Xie, T.; Sun, S. H.; Meng, G. W.; Zhang, L. D. *Appl. Phys. Lett.* **2003**, *82*, 4791.

(23) Shen, G.; Cho, J. H.; Yoo, J. K.; Yi, G. C.; Lee, C. J. *J. Phys. Chem. B* **2005**, *109*, 5491-5496.

(24) Vanheusden, K.; Warren, W. L.; Seager, C. H.; Tallant, D. R.; Voigt, J. A.; Gnade, B. E. *J. Appl. Phys.* **1996**, *79*, 7983.

(25) van Dijken, A.; Meulenkamp, E. A.; Vanmaekelbergh, D. e. l.; Meijerink, A. *J. Phys. Chem. B* **2000**, *104*, 1715.

(26) Li, D.; Leung, Y. H.; Djurisic, A. B.; Liu, Z. T.; Xie, M. H.; Shi, S. L.; Xu, S. J.; Chan, W. K. *Appl. Phys. Lett.* **2004**, *85*, 1601-1603.

(27) Djurisic, A. B.; Leung, Y. H.; Choy, W. C. H.; Cheah, K. W.; Chan, W. K. *Appl. Phys. Lett.* **2004**, *84*, 2635-2637.

(28) Wyszecki, G.; Stiles, W. S. *Color science: concepts and methods, quantitative data and formulae*; 2nd ed.; Wiley: New York, 1982.

(29) Zhang, Y.; Russo, R. E.; Mao, S. S. *Appl. Phys. Lett.* **2005**, *87*, 043106.

(30) Yen, W. M.; Weber, M. J. *Inorganic Phosphors: Compositions, Preparation and Optical Properties*; CRC Press, 2004; Vol. 20.

(31) In Figure 3A the apparent rise times differ slightly due to intentional changes in the streak camera's time resolution (110 ps for micropowder, 50 ps for doped micropowder, 30 ps for nanowires). In all cases the rise times are instrument-limited.

(32) Studenikin, S. A.; Cocivera, M. *J. Appl. Phys.* **2002**, *91*, 5060.

SYNOPSIS TOC GRAPHIC: